Applied Physics Letters

Strain-facilitated process for the lift-off of a Si layer of less than 20 nm thickness

Cite as: Appl. Phys. Lett. **87**, 251907 (2005); https://doi.org/10.1063/1.2146211
Submitted: 22 September 2005 . Accepted: 03 November 2005 . Published Online: 12 December 2005

Lin Shao, Yuan Lin, J. G. Swadener, J. K. Lee, Q. X. Jia, Y. Q. Wang, M. Nastasi, Phillip E. Thompson, N. David Theodore, T. L. Alford, J. W. Mayer, Peng Chen, and S. S. Lau

Strain-facilitated process for the lift-off of a Si layer of less than 20 nm thickness

Lin Shao,[a] Yuan Lin, J. G. Swadener, J. K. Lee, Q. X. Jia, Y. Q. Wang, and M. Nastasi
Los Alamos National Laboratory, Los Alamos, New Mexico 87545

Phillip E. Thompson
Code 6812, Naval Research Laboratory, Washington, DC 20375-5347

N. David Theodore
Advanced Products Research and Development Laboratory, Freescale Semiconductor Inc., Tempe, Arizona 85284

T. L. Alford and J. W. Mayer
Department of Chemical and Materials Engineering, Arizona State University, Tempe, Arizona 85287

Peng Chen and S. S. Lau
University of California at San Diego, La Jolla, California 92093

(Received 22 September 2005; accepted 3 November 2005; published online 12 December 2005)

We report a process for the lift-off of an ultrathin Si layer. By plasma hydrogenation of a molecular-beam-epitaxy-grown heterostructure of Si/Sb-doped-Si/Si, ultrashallow cracking is controlled to occur at the depth of the Sb-doped layer. Prior to hydrogenation, an oxygen plasma treatment is used to induce the formation of a thin oxide layer on the surface of the heterostructure. Chemical etching of the surface oxide layer after hydrogenation further thins the thickness of the separated Si layer to be only 15 nm. Mechanisms of hydrogen trapping and strain-facilitated cracking are discussed. © *2005 American Institute of Physics*. [DOI: 10.1063/1.2146211]

Driven by the need for faster and smaller microprocessors with lower power consumption, silicon-on-insulator (SOI) wafers have now been established as a substrate choice for next generation devices.[1] According to the international technology roadmap for semiconductors, fabrication of fully depleted metal-oxide semiconductors beyond 90 nm nodes will require ultrathin SOI wafers with top Si layers that are less than 20 nm thick.[2] In the conventional ion-cut technique (Smart-cut™) for SOI production, hydrogen ion implantation, and thermal annealing are used to induce layer splitting at a depth which is controllable by adjusting the energy of hydrogen ion implantation.[3] This technique, however, is unable to transfer a layer less than 20 nm thick even if ultralow energy hydrogen ion implantation is used.[4] Extensive efforts have been made to optimize the existing process and to develop alternative approaches for ultrathin layer transfer. One method is to introduce H trapping centers either by dopant ion implantation,[5] or heavy ion implantation.[6] The thinnest layer transfer reported for this kind of approach is 75 nm.[6]

In this work we report an approach for transferring Si layers with less than 20 nm thickness. This method of layer transfer is based on the following processes: (1) hydrogenation, instead of hydrogen ion implantation, is used to introduce H atoms; (2) the location of splitting is controlled by the depth of a heavily Sb-doped Si layer formed by film growth; and (3) before hydrogenation, an oxygen plasma treatment is performed to induce formation of a surface silicon oxide layer. This layer can be etched away later to thin the layer to be transferred or left in place to assist with the bonding process.

Our experiments started with molecular beam epitaxial growth of two monocrystalline (001) Si samples, each containing a 3-nm-thick Sb-doped Si layer at a depth of 50 nm, or 90 nm, beneath the surface. Immediately after an oxygen plasma treatment, both samples were subjected to plasma hydrogenation at a temperature of around 200–300 °C, in an inductively coupled plasma system with a bias of around 400 V. Some of the hydrogenated samples were dipped into a 10% diluted hydrofluoric solution for 10 s to etch the surface oxide layers. For purposes of comparison, a control Si sample without Sb doping was included in all process steps.

Transmission electron microscopy (TEM) and Rutherford backscattering spectrometry (RBS) were used to characterize the sample structures. A focused ion-beam lift-off method was used to prepare the TEM samples. Imaging was performed using parallel illumination, with a Philips CM200 field-emission gun TEM operated at an accelerating voltage of 200 kV. RBS analysis was performed using a 2.0 MeV $^4He^+$ analyzing beam with a surface barrier detector positioned 167° away from the incident beam. The sample was tilted 75° to increase the RBS depth resolution. Depth profiles of elements of interest were measured with secondary ion mass spectrometry (SIMS) by using a 1 keV Cs^+ beam. The strain in the samples was obtained from high resolution x-ray diffraction (XRD) data in conjunction with Bede RADS autofit software. An $\omega-2\theta$ scan around Si (004) was collected using a Bede D1 x-ray diffractometer. In the fitting procedure the samples were modeled as a multilayer structure. Through this process the lattice parameter of each layer was successively determined by fitting the model to the diffraction data, thereby producing a strain depth profile. High-resolution strain data can be obtained by setting the thickness of each layer in the multilayer structure at the angstrom level.

Figures 1(a)–1(c) present cross-section TEM micrographs of Sb-doped Si with a 90-nm-thick Si capping layer,

[a]Electronic mail: lshao@mailaps.org

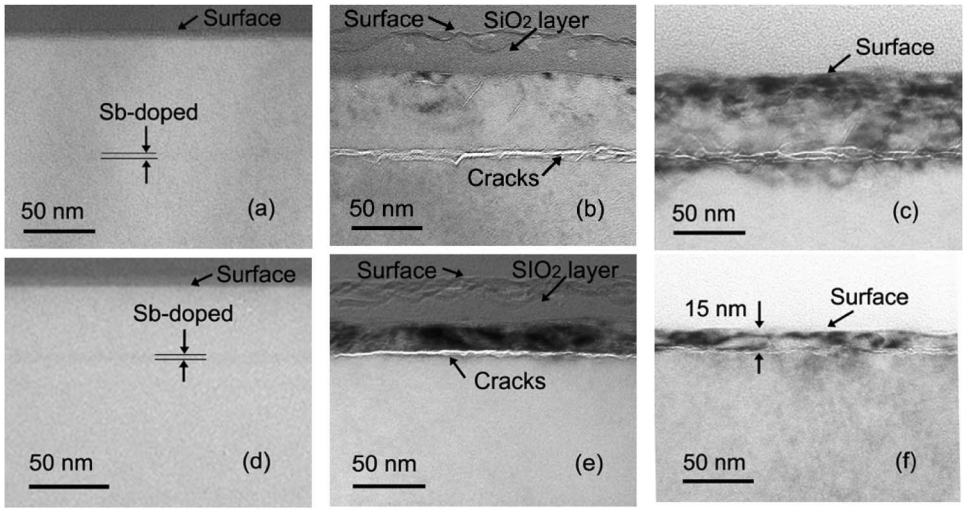

FIG. 1. TEM micrographs obtained from: (a) as-grown Si containing a Sb-doped layer at a depth of 90 nm, (b) after hydrogenation, (c) after chemical etching, (d) as-grown Si containing a Sb-doped layer at a depth of 50 nm, (e) after hydrogenation, and (f) after chemical etching.

at different process stages. Figures 1(d)–1(f) show another set of samples with a 50-nm-thick Si capping layer. For as-grown samples [Figs. 1(a) and 1(d)], the positions of the buried Sb-doped layers are marked. After the hydrogenation, amorphous surface layers, about 30 nm thick, are formed on both samples [Figs. 1(b) and 1(e)]. RBS confirmed that these layers are composed of $SiO_{2\pm0.1}$ (to be discussed later). Furthermore, (111)-oriented platelets are observed beneath the surface oxide layers. In both samples, continuous (100)-oriented cracks, which are parallel to the Si surfaces, are formed at the depth of the Sb-doped layers. After chemical etching, the surface oxide layers are removed [Figs. 1(c) and 1(f)]. As shown in Fig. 1(f), the resulting thickness of the residual top Si layer is only about 15 nm.

Figure 2 compares random RBS spectra from the Sb-doped Si sample (90 nm deep) before and after chemical etching. The composition of the hydrogenated sample, as a function of depth, was extracted by fitting the RBS spectra using a commercial simulation software RUMP.[7] The simulated spectra are depicted by solid lines in Fig. 2. For the sample before chemical etching, RBS reveals that its outer layer, about 34 nm thick, has a composition of $SiO_{2\pm0.1}$. The error bar is estimated from the fitting. The absence of an O signal in the etched sample indicates that the oxide layer has been totally removed after the etching. Interestingly, both the experimental data as well as the simulation, as shown in the insert of Fig. 2, reveal two Sb peaks, one corresponding to the originally doped Sb layer and another corresponding to a buildup of Sb at the interface between the oxide layer and the Si layer. Such Sb buildup is not observed in the as-grown sample (not shown).

Figures 3(a) and 3(b) present SIMS profiles obtained from the Sb-doped samples after hydrogenation. Box-like distributions of O atoms are revealed within the top 34 nm of both samples. The SIMS data also show Sb buildup at the interface between the oxide and Si layers. These data agree well with the composition information obtained from RBS measurements. The Sb buildup at the oxide-to-silicon interface is the result of diffusion and segregation. First, during molecular-beam-epitaxy (MBE) growth of the heavily Sb-doped Si layer, Sb out diffuses into the Si layer during its growth, resulting in moderate Sb doping of the Si layer. Second, during the surface oxidation, Sb atoms segregate out of the growing oxide layer, resulting in a buildup of Sb within the silicon adjacent to the oxide interface. This segregation mechanism, also called the "snow plow effect," happens for dopants (e.g., P, As, or Sb) which have a lower solubility in silicon oxide than in Si.[8]

As shown in Figs. 3(a) and 3(b), the H concentration profiles peak at the depths corresponding to the peak concen-

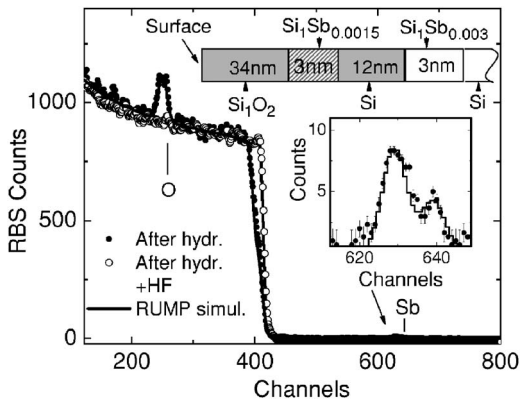

FIG. 2. Random RBS spectra obtained from hydrogenated Si containing a Sb-doped layer at a depth of 90 nm and the same sample after chemical etching. The inset shows a locally enlarged profile of the Sb signals.

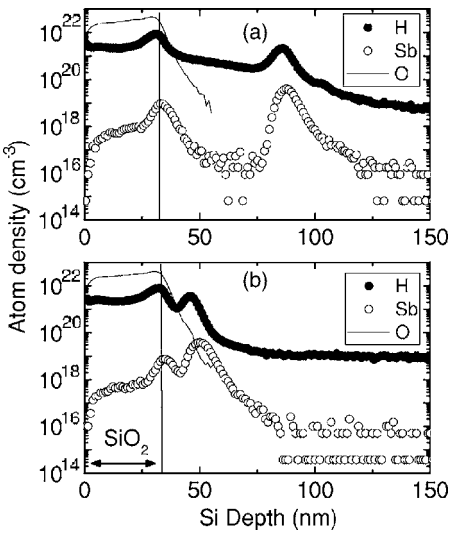

FIG. 3. SIMS profiles showing O, H, and Sb in hydrogenated Si containing a 3-nm-thick Sb-doped layer at a depth of (a) 90 and (b) 50 nm.

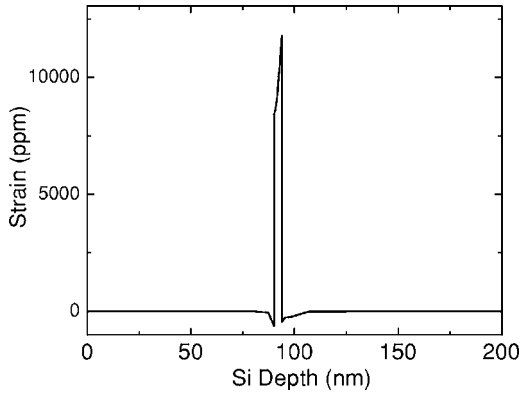

FIG. 4. Out-of-plane strain as a function of depth in as-grown Si containing a Sb-doped layer at a depth of 90 nm. The profile was deduced from x-ray diffraction measurements.

trations of Sb. In order to confirm that the observed H trapping is not a SIMS artifact due to the H ionization yield changes in the Sb doped regions, we have performed elastic recoil detection (ERD) analysis on hydrogenated samples. H ERD profiles (not shown) clearly confirmed the two H peaks observed in Fig. 3(a). Multiple trapping of H in *n*-type Si has been previously reported.[9,10] It was proposed that large SbH_n complexes ($n \geqslant 2$) are formed through trapping of additional H by SbH complexes.[10] However, the basic mechanism for formation of SbH complexes is still being debated. Rizk *et al.* suggested that formation of H-donor complexes is a consequence of compensation between negative H^- ions and positively ionized donors.[11] Pantelides, however, suggested that in *n*-type Si donors are paired with neutral H^0 ions since H has only a donor level in the gap.[12]

The H trapping by Sb cannot by itself explain the continuous (100)-oriented cracks observed at the original Sb-doped layer. It is believed that strain plays an important role in crack formation. Figure 4 shows a strain-depth profile obtained from the as-grown Sb-doped Si, using XRD. At the depth of the Sb-doped layer (~90 nm), a sharp out-of-plane tensile strain is observed, which indicates a Poisson's effect from in-plane compressive strains.[13] On the other hand, out-of-plane compressive strains are observed in the Si residing on both sides of the Sb layer. The presence of opposing strains on either side of the interface between the Si and the Sb-doped layer places the interface in a state of shear.

Strain can facilitate (100)-oriented platelet formation and cracking.[14] First, agglomeration of vacancies is kinetically preferred in regions of in-plane compressive strain. This effect has been previously observed in compressively strained SiGe layers.[15] Second, interactions of H with those vacancies which are agglomerated along (100) planes facilitate the formation of (100)-orientated platelets. Various studies have proposed that vacancies play a central role in platelet formation.[16–18] Third, cracking along (100) planes is facilitated by the presence of an interfacial shear strain. The shear strain can provide added forces to break Si bonds at the cracking fronts of (100) oriented platelets.[19]

By confining crack propagation to extend along the strained interface between Si and the Sb-doped layer, the zigzag networking of microcracks is minimized. It is expected therefore that the smoothness of the transfer layer can be enhanced. In the current study, the surface oxide layer is etched away. This oxide layer, can, however, be left in place and be directly bonded to a thermal oxidized wafer, thereby assisting in the transfer of an ultrathin layer that is only 15 nm thick. Sb segregation at the Si/SiO_2 interface can be an issue for device fabrication. Sb aggregation can be reduced by reducing the MBE growth temperature and/or by reducing the Sb doping level for H trapping.

In summary, we have shown that a buried Sb-doped layer in Si can be used to provide H trapping centers during hydrogenation and thereby facilitate the transfer of a thin Si layer. Continuous cracking following hydrogenation is controlled to occur at the Sb-doped layer. Furthermore, the thickness of the to-be-transferred Si layer can be reduced by forming a surface oxide layer, which can then be chemically etched away. This method of layer transfer is free of ion implantation steps.

This research is supported by the Department of Energy, Office of Basic Energy Science, and in part by the Office of Naval Research. UCSD and ASU gratefully acknowledge sponsorship from National Science Foundation (DMR-0308127, L. Hess).

[1] J. P. Collinge, *Silicon-on-Insulator Technology: Materials to VLSI* (Kluwer Academic, Boston, 1991).
[2] International Technology Roadmap for Semiconductors, 2003 ed., http://public.itrs.net.
[3] M. Bruel, Nucl. Instrum. Methods Phys. Res. B **108**, 313 (1996).
[4] O. Moutanabbir, A. Giguère, and B. Terreault, Appl. Phys. Lett. **84**, 3286 (2004).
[5] P. Chen, P. K. Chu, T. Höchbauer, J.-K. Lee, M. Nastasi, D. Buca, S. Mantl, R. Loo, M. Caymax, T. Alford, J. W. Mayer, N. D. Theodore, M. Cai, B. Schmidt, and S. S. Lau, Appl. Phys. Lett. **86**, 031904 (2005).
[6] A. Usenko, J. Electron. Mater. **32**, 872 (2003).
[7] An updated version of RUMP can be downloaded from http://www.genplot.com.
[8] S. Wolf and R. N. Tauber, *Silicon Processing for The VLSI Era, Volume 1—Process Technology* (Lattice, Sunset Beach, CA, 1986).
[9] N. M. Johnson, C. Herring, and D. J. Chadi, Phys. Rev. Lett. **56**, 769 (1986).
[10] Z. N. Liang, C. Haas, and L. Nielsen, Phys. Rev. Lett. **72**, 1846 (1994).
[11] R. Rizk, P. de Mierry, D. Ballutaud, M. Aucouturier, and D. Mthiot, Phys. Rev. B **44**, 6141 (1991).
[12] S. T. Pantelides, Appl. Phys. Lett. **50**, 995 (1987).
[13] H. Tada, P. C. Paris, and G. R. Irwin, *The Stress Analysis of Cracks Handbook* (Del Research Corp., Hellertown, PA, 1985).
[14] L. Shao, Y. Lin, J. K. Lee, Q. X. Jia, Y. Q. Wang, M. Nastasi, P. E. Thompson, N. David Theodore, P. K. Chu, T. L. Alford, J. W. Mayer, P. Chen, and S. S. Lau, Appl. Phys. Lett. **87**, 091902 (2005).
[15] L. Fedina, O. I. Lebedev, G. Van Tendeloo, J. Van Landuyt, O. A. Mironov, and E. H. C. Parker, Phys. Rev. B **61**, 10336 (2000).
[16] M. K. Weldon, V. E. Marsico, Y. J. Chabal, A. Agarwal, D. J. Eaglesham, J. Sapjeta, W. L. Brown, D. C. Jacobson, Y. Caudano, S. B. Christman, and E. E. Chaban, J. Vac. Sci. Technol. B **15**, 1065 (1997).
[17] M. Nastasi, T. Höchbauer, J. K. Lee, A. Misra, J. P. Hirth, M. Ridgway, and T. Lafford, Appl. Phys. Lett. **86**, 154102 (2005).
[18] F. A. Reboredo, M. Ferconi, and S. T. Pantelides, Phys. Rev. Lett. **82**, 4870 (1999).
[19] L. Shao, Y. Lin, J. G. Swadener, J. K. Lee, Q. X. Jia, Y. Q. Wang, M. Nastasi, P. E. Thompson, N. David Theodore, T. L. Alford, J. W. Mayer, P. Chen, and S. S. Lau (unpublished).